PROCEEDINGS OF THE ROYAL SOCIETY A

rspa.royalsocietypublishing.org

Research

Cite this article: Neukirch S, Antkowiak A, Marigo J-J. 2013 The bending of an elastic beam by a liquid drop: a variational approach. Proc R Soc A 469: 20130066.
http://dx.doi.org/10.1098/rspa.2013.0066

Received: 1 February 2013
Accepted: 5 June 2013

Subject Areas:
mechanical engineering, fluid mechanics, mathematical modelling

Keywords:
capillarity, one-dimensional elasticity, bifurcation, irreversibility

Author for correspondence:
Sébastien Neukirch
e-mail: sebastien.neukirch@upmc.fr

The bending of an elastic beam by a liquid drop: a variational approach

Sébastien Neukirch[1,2], Arnaud Antkowiak[1,2] and Jean-Jacques Marigo[3]

[1]CNRS, UMR 7190, Institut Jean Le Rond d'Alembert, 75005 Paris, France
[2]UPMC Univ Paris 06, UMR 7190, Institut Jean Le Rond d'Alembert, 75005 Paris, France
[3]CNRS, Ecole Polytechnique, UMR 7649, Lab. Méca. Solides, 91128 Palaiseau Cedex, France

We study the interaction of a liquid drop with an elastic beam in the case where bending effects dominate. We use a variational approach to derive equilibrium equations for the system in the presence of gravity and in the presence or absence of contact line pinning. We show that the derived equilibrium equations for the beam subsystem reveal the external forces applied on the beam by the liquid and vapour phases. Among these, the force applied at the triple line (the curve where the three phases meet) is found to lie along the liquid–vapour interface.

1. Introduction

The present trend towards miniaturization of engineering systems and machines is giving surface effects the leading role: in a system of size L, the respective scalings of volume (L^3) and surface (L^2) forces are such that the latter outrange the former as soon as L is small enough. Among other surface effects, surface tension is now widely used at small scales, for example, to self-assemble microsystems [1]. The concept of force is not easy to explain to recalcitrant students: has anyone already seen a force? How to be sure of the direction of an applied force? Capillary forces are no exception, and conceptual questions about it recurrently emerge [2]. These capillary forces are now used to bend small elastic structures [3], and it has been previously shown that under certain conditions water droplets could be encapsulated by elastic strips [4–6]. In these works, models were derived

using a force approach where the capillary force applied on the beam at menisci was assumed to be along the liquid–air interface. This assumption has recently been questioned [7], and to investigate the matter, we here study the interaction of a liquid drop with a flexible beam from an energy point of view. In particular, we derive equilibrium equations of the system from a variational approach that is merely built on the classical hypothesis of the presence of surface energies arising at interfaces between the three phases: solid, liquid and vapour. As a refinement to previous works, we here also consider the hydrostatic pressure in the liquid drop and show how the interacting equations for the shape of the liquid–air interface and the elastic beam are solved simultaneously.

In §2, we recall that the Young–Dupré relation for the contact angle of a drop lying on a substrate can be derived from a variational approach where the concept of force is not invoked, as first realized by Gauss [8,9] and see also Kirchhoff [10]. In §3, we consider the case where the substrate is a flexible beam, and we add gravity (for the beam and the liquid) in §4. In §5, we extend our model to the case of contact line pinning and we finally illustrate our results by computing the behaviour of a drop-beam system as the drop evaporates. Conclusion follows in §6.

2. Liquid drop on rigid substrate, no gravity

We consider the equilibrium of a liquid drop of given volume sitting on a rigid substrate of length L (figure 1). If the drop is small enough, then gravity and the hydrostatic part of the pressure can be neglected, and consequently, the liquid–air interface is circular. For the sake of simplicity, we adopt a two-dimensional framework where the liquid–vapour interface is a cylindrical arc (figure 1*a*). This two-dimensional approximation has been used in Antkowiak *et al.* [5] and Rivetti & Neukirch [6] where it has been shown to reasonably reproduce experimental data. We call r its radius, w its height and 2β its opening angle. The liquid–vapour interface then comprises (i) a cylindrical surface of area $2\beta rw$, and (ii) two planar caps, each of area $A = r^2(\beta - \sin\beta\cos\beta)$. The wetting angle is equal to β, and the wetted length of the beam is noted $2D$. To each of the three different interfaces, liquid–solid, liquid–vapour and solid–vapour, we associate an energy per area: $\gamma_{\ell s}$, $\gamma_{\ell v}$ and γ_{sv}, respectively. The energy of the system is then given by the sum:

$$E(\beta, r, D) = 2(w\beta r + A)\gamma_{\ell v} + 2wD\gamma_{\ell s} + 2w(2L - D)\gamma_{sv}. \tag{2.1}$$

To minimize E under the constraints of (i) fixed volume $V = Aw = wr^2(\beta - \sin\beta\cos\beta)$, and (ii) geometric relation $D = r\sin\beta$, we then introduce the Lagrangian:

$$\mathcal{L} = E - \eta w(2D - 2r\sin\beta) - \mu w[r^2(\beta - \sin\beta\cos\beta)], \tag{2.2}$$

where η and μ are Lagrange multipliers. We note $\gamma = \gamma_{\ell v}$ and $\Delta\gamma = \gamma_{\ell s} - \gamma_{sv}$. Equilibrium equations are found by imposing that derivatives of $\mathcal{L}$ with regard to the three variables β, r, D vanish

$$\frac{\partial \mathcal{L}}{\partial \beta} = 0 = 2wr\gamma + 2\eta wr\cos\beta - \mu wr^2(1 - \cos 2\beta), \tag{2.3a}$$

$$\frac{\partial \mathcal{L}}{\partial r} = 0 = 2w\beta\gamma + 2\eta w\sin\beta - 2\mu wr(\beta - \sin\beta\cos\beta) \tag{2.3b}$$

and

$$\frac{\partial \mathcal{L}}{\partial D} = 0 = 2w\Delta\gamma - 2\eta w. \tag{2.3c}$$

Combining (2.3*a*) $\cos\beta$ + (2.3*b*) $r\sin\beta$ and (2.3*a*) $\sin\beta$ − (2.3*b*) $r\cos\beta$ yields $\gamma = \mu r$ and $\gamma\cos\beta + \eta = 0$, and using (2.3*c*) gives $\eta = \Delta\gamma$. We finally arrive at

$$\Delta\gamma + \gamma\cos\beta = 0 \tag{2.4}$$

and

$$\mu = \frac{\gamma}{r}. \tag{2.5}$$

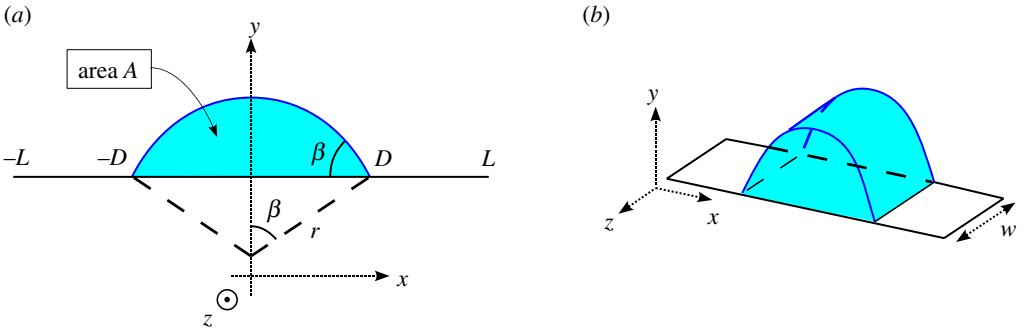

Figure 1. (*a*, *b*) A two-dimensional model of a liquid drop at rest on a rigid substrate. In the absence of gravity, the liquid–vapour interface is a circular arc of radius r. The contact angle β is set by the balance of the interfaces energies, see equation (2.5), and the wetted length $2D$ depends on the drop volume V. (Online version in colour.)

The first equation is the well-known Young–Dupré relation giving the contact angle and can be interpreted as a force balance of the triple point in the horizontal direction. The second equation gives the Laplace pressure inside the liquid drop. In the vertical direction, force balance is also achieved: the vertical forces acting on the rigid substrate are the distributed Laplace pressure μ and the surface tension $\gamma_{\ell v}$, with the total downward force being $2Dw\mu$ and the total upward force being $2\gamma_{\ell v}\sin\beta$. Using (2.5) and $D = r\sin\beta$, we see that these two forces equilibrate. We shall see in §3 that when the substrate is a thin elastic strip, these forces induce flexural deformations.

3. Liquid drop on a flexible beam, no gravity

We now consider the case of a liquid drop sitting on an elastic strip (figure 2), and we look for equilibrium equations governing the bending of the elastic strip by capillary forces. We still work under the hypothesis where gravity and the hydrostatic part of the pressure can be neglected, yielding a circular liquid–air interface. In addition to the sum of the three interface energies:

$$E_\gamma = 2(w\beta r + A)\gamma_{\ell \mathrm{v}} + 2wD\gamma_{\ell \mathrm{s}} + 2w(2L - D)\gamma_{\mathrm{sv}} \tag{3.1}$$

we consider the bending energy of the elastic strip. We use the arc-length s along the strip to parametrize its current position $\boldsymbol{r}(s) = (x(s), y(s))$. The unit tangent, $\boldsymbol{t}(s) = \mathrm{d}\boldsymbol{r}/\mathrm{d}s$, makes an angle $\theta(s)$ with the horizontal axis: $\boldsymbol{t} = (\cos\theta(s), \sin\theta(s))$. The bending energy density is proportional to the square of the curvature $\theta'(s)$:

$$E_\kappa = \frac{1}{2}YI\int_{-L}^{L}[\theta'(s)]^2\,\mathrm{d}s, \tag{3.2}$$

where YI is the bending rigidity of the strip (Y is Young's modulus of the beam material, and $I = h^3w/12$ is the second moment of area of the section of the beam). We minimize $E = E_\kappa + E_\gamma$ under the following four constraints. First, the liquid volume V is fixed. It is given by $V = wA$, where A is the area in between the liquid–air interface and the liquid–solid interface:

$$A = r^2\left(\beta - \frac{1}{2}\sin 2\beta\right) + 2x(D)y(D) - \int_{x(-D)}^{x(D)} y\,\mathrm{d}x. \tag{3.3}$$

Second, we have the geometric constraint:

$$x(D) = r\sin\beta \tag{3.4}$$

that is due to the intersection of the circular liquid–vapour interface and the beam at $s = D$. As the variables $x(s)$, $y(s)$ and $\theta(s)$ all appear in the present formulation, we have to consider the

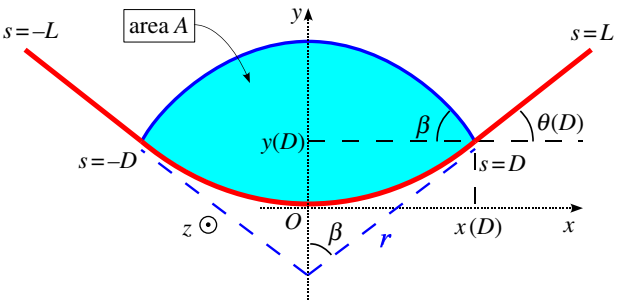

Figure 2. An elastic strip bent by capillary forces. In the absence of gravity, the liquid–vapour interface is a circular arc, and the strip outside the interaction region is straight. The system is invariant is the z-direction, with width w. (Online version in colour.)

continuous constraints relating them. These are our third and fourth constraints:

$$x'(s) = \cos\theta(s), \quad y'(s) = \sin\theta(s). \tag{3.5}$$

These continuous constraints necessitate the use of varying Lagrange multipliers $\nu(s)$ and $\lambda(s)$. We therefore introduce the Lagrangian:

$$\mathcal{L} = E_\kappa + E_\gamma - \mu w\left[r^2\left(\beta - \frac{1}{2}\sin 2\beta\right) + 2x(D)y(D) - \int_{-D}^{D} yx'\,\mathrm{d}s\right] - \eta w[x(D) - r\sin\beta] + \int_{-L}^{L}\nu(s)[x' - \cos\theta]\,\mathrm{d}s + \int_{-L}^{L}\lambda(s)[y' - \sin\theta]\,\mathrm{d}s. \tag{3.6}$$

As we will treat only symmetric solutions, we focus on the positive s interval: $s \in [0; L]$ with the following boundary conditions:

$$x(0) = 0, \quad y(0) = 0, \quad \theta(0) = 0. \tag{3.7}$$

We also remark that in this elastica model, the varying Lagrange multiplier $\nu(s)$ and $\lambda(s)$ will be found to be the internal force components (appendix A). As the external force coming for the meniscus will make the internal force discontinuous as s passes through $s = D$, we split the two last integrals in the Lagrangian (3.6) and write:

$$s \in [0; D) : \nu(s) = \nu_i(s), \quad \lambda(s) = \lambda_i(s) \tag{3.8}$$

and

$$s \in (D; L] : \nu(s) = \nu_e(s), \quad \lambda(s) = \lambda_e(s). \tag{3.9}$$

Dropping out constant terms, we arrive at:

$$\begin{aligned}\mathcal{L}(x, y, \theta, \beta, r, D) = {} & \frac{1}{2}\gamma I\int_0^L [\theta'(s)]^2\,\mathrm{d}s + w\beta r\gamma + wD\Delta\gamma - \eta w\left[\int_0^D x'\,\mathrm{d}s - r\sin\beta\right] \\ & - \mu w\left[\frac{r^2}{2}\left(\beta - \frac{1}{2}\sin 2\beta\right) + \int_0^D x'\,\mathrm{d}s \times \int_0^D y'\,\mathrm{d}s - \int_0^D yx'\,\mathrm{d}s\right] \\ & + \int_0^D \nu_i(s)[x' - \cos\theta]\,\mathrm{d}s + \int_D^L \nu_e(s)[x' - \cos\theta]\,\mathrm{d}s \\ & + \int_0^D \lambda_i(s)[y' - \sin\theta]\,\mathrm{d}s + \int_D^L \lambda_e(s)[y' - \sin\theta]\,\mathrm{d}s,\end{aligned} \tag{3.10}$$

where $\gamma = \gamma_{\ell v}$ and $\Delta\gamma = \gamma_{\ell s} - \gamma_{sv}$.

(a) First variation

The energy E and the Lagrangian $\mathcal{L}$ are functions of the variables $x, y, \theta, \beta, r, D$. We note $X = (x, y, \theta, \beta, r, D)$ and we consider the conditions for the state X_e to minimize the energy E. Calculus of variation shows that a necessary condition is

$$\mathcal{L}'(X_e)(\bar{X}) = \frac{\mathrm{d}}{\mathrm{d}\epsilon}\mathcal{L}(X_e + \epsilon\bar{X})\Big|_{\epsilon=0} = 0, \tag{3.11}$$

where $\bar{X} = (\bar{x}, \bar{y}, \bar{\theta}, \bar{\beta}, \bar{r}, \bar{D})$. Moreover, boundary conditions (3.7) imply that $\bar{x}(0) = 0$, $\bar{y}(0) = 0$, $\bar{\theta}(0) = 0$. Noting that:

$$\int_0^{A+\epsilon\bar{A}} f(x)\,\mathrm{d}x = \int_0^A f(x)\,\mathrm{d}x + \epsilon\bar{A}f(A) + O(\epsilon^2) \tag{3.12}$$

we evaluate the first variation (3.11) to be

$$\begin{aligned}
\mathcal{L}'(X_e)(\bar{X}) = {} & YI\int_0^L \theta'\bar{\theta}'\,\mathrm{d}s + w\beta\bar{r}\gamma + w\bar{\beta}r\gamma + w\bar{D}\Delta\gamma - \mu w\left[r\bar{r}\left(\beta - \frac{1}{2}\sin 2\beta\right) + \frac{\bar{\beta}r^2}{2}(1 - \cos 2\beta)\right] \\
& - \mu w\left[\int_0^D \bar{x}'\,\mathrm{d}s \times \int_0^D y'\,\mathrm{d}s + \int_0^D x'\,\mathrm{d}s \times \int_0^D \bar{y}'\,\mathrm{d}s + \bar{D}x'(D)y(D) + \bar{D}x(D)y'(D)\right] \\
& + \mu w\left[\int_0^D \bar{y}x'\,\mathrm{d}s + \int_0^D y\bar{x}'\,\mathrm{d}s + \bar{D}y(D)x'(D)\right] \\
& - \eta w\left[\int_0^D \bar{x}'\,\mathrm{d}s + \bar{D}x'(D) - \bar{r}\sin\beta - r\bar{\beta}\cos\beta\right] \\
& + \int_0^D \nu_i(s)[\bar{x}' + \bar{\theta}\sin\theta]\,\mathrm{d}s + \int_D^L \nu_e(s)[\bar{x}' + \bar{\theta}\sin\theta]\,\mathrm{d}s \\
& + \int_0^D \lambda_i(s)[\bar{y}' - \bar{\theta}\cos\theta]\,\mathrm{d}s + \int_D^L \lambda_e(s)[\bar{y}' - \bar{\theta}\cos\theta]\,\mathrm{d}s
\end{aligned} \tag{3.13}$$

where we have used (3.5) at $s = D$ to eliminate some terms related to the last four integrals. We require this expression to vanish for all $\bar{x}(s)$, $\bar{y}(s)$, $\bar{\theta}(s)$, $\bar{\beta}$, $\bar{r}$ and $\bar{D}$. For (3.13) to vanish for all $\bar{\beta}$, we must have, as before

$$rw\gamma - \mu w\frac{r^2}{2}(1 - \cos 2\beta) + \eta wr\cos\beta = 0. \tag{3.14}$$

For (3.13) to vanish for all $\bar{r}$, we must have, as before:

$$\beta w\gamma - \mu wr(\beta - \sin\beta\cos\beta) + \eta w\sin\beta = 0. \tag{3.15}$$

Combining these last two equations, we obtain:

$$\mu r = \gamma \quad \text{and} \quad \gamma\cos\beta + \eta = 0, \tag{3.16}$$

where μ is identified to the Laplace pressure. For (3.13) to vanish for all $\bar{D}$, we must have:

$$w\Delta\gamma - \mu wx(D)y'(D) - \eta wx'(D) = 0. \tag{3.17}$$

Using (3.4), (3.5) and (3.16), we obtain:

$$\Delta\gamma + \gamma\cos[\beta + \theta(D)] = 0. \tag{3.18}$$

This is the Young–Dupré relation for the wetting angle $\beta + \theta(D)$ between the beam and the liquid–air meniscus. Requiring (3.13) to vanish for all $\bar{\theta}$ yields, after integration by parts:

$$\begin{aligned}
& YI[\theta'\bar{\theta}]_0^D + \int_0^D [-YI\theta'' + \nu_i\sin\theta - \lambda_i\cos\theta]\bar{\theta}\,\mathrm{d}s \\
& + YI[\theta'\bar{\theta}]_D^L + \int_D^L [-YI\theta'' + \nu_e\sin\theta - \lambda_e\cos\theta]\bar{\theta}\,\mathrm{d}s = 0
\end{aligned} \tag{3.19}$$

which implies that the curvature $\theta'(s)$ is continuous as s goes through D and that it vanishes at the $s = L$ extremity. Moreover, we obtain the moment equilibrium equations:

$$YI\theta'' = \nu_i \sin\theta - \lambda_i \cos\theta \quad \text{for } s \in [0; D) \tag{3.20}$$

and

$$YI\theta'' = \nu_e \sin\theta - \lambda_e \cos\theta \quad \text{for } s \in (D; L], \tag{3.21}$$

where we see that the continuous Lagrange multipliers $\nu(s)$, and $\lambda(s)$ can be identified as the x and y components of the internal force: $n_x \equiv \nu$ and $n_y \equiv \lambda$. Requiring (3.13) to vanish for all $\bar{x}$ yields, after integration by parts:

$$[(-\mu w(y(D) - y) - \eta w + \nu_i)\bar{x}]_0^D - \int_0^D (\mu w y' + \nu_i')\bar{x}\,\mathrm{d}s + [\nu_e \bar{x}]_D^L - \int_D^L \nu_e'\bar{x}\,\mathrm{d}s = 0. \tag{3.22}$$

The fact that we have $\bar{x}(0) = 0$, but arbitrary $\bar{x}(D)$ and $\bar{x}(L)$ implies

$$\nu_e(L) = 0, \quad \nu_e(D) - \nu_i(D) = -\eta w, \quad \nu_e' = 0, \quad \nu_i' = -\mu w y'. \tag{3.23}$$

Requiring (3.13) to vanish for all $\bar{y}$ similarly implies

$$\lambda_e(L) = 0, \quad \lambda_e(D) - \lambda_i(D) = -\mu w x(D), \quad \lambda_e' = 0, \quad \lambda_i' = \mu w x', \tag{3.24}$$

where we see that Laplace pressure generates an outward normal force $\mu w(y', -x')$ that causes the internal force (ν_i, λ_i) to vary. In addition, we see that the internal force vanishes at the $s = L$ extremity and that it experiences a discontinuity at $s = D$. Using (3.4) and (3.16) we find that:

$$\begin{pmatrix} \nu_e(D) \\ \lambda_e(D) \end{pmatrix} - \begin{pmatrix} \nu_i(D) \\ \lambda_i(D) \end{pmatrix} = \gamma w \begin{pmatrix} \cos\beta \\ -\sin\beta \end{pmatrix} \tag{3.25}$$

is the external force applied on the beam at $s = D$ is along the meniscus, as used in Neukirch *et al.* [11] and Antkowiak *et al.* [5].

Once γ, $\Delta\gamma$, YI and the volume V are set, the equilibrium configuration is found by solving the nonlinear boundary value problem for $s \in (0; D)$, given by equations (3.5), (3.20), (3.21), (3.23) and (3.24), with left boundary conditions (3.7) and right boundary conditions $\theta'(D) = 0$, $\nu_i(D) = -\gamma w \cos\beta$ and $\lambda_i(D) = \gamma w \sin\beta$. The presence of unknown parameters β, r and D is balanced by additional conditions (3.3), (3.4) and (3.18).

We remark that, as in the case of a rigid substrate (§2), the sum of the distributed Laplace pressure $f_1 = \int_0^D -\mu w x'\,\mathrm{d}s$ applied along the y-axis on the beam (equation (3.24)) is balanced by the y component of the meniscus force at $s = D$: $f_2 = \gamma w \sin\beta$, that is $f_1 + f_2 = 0$.

(b) Equilibrium solutions

We now solve the boundary value problem for different values of the parameters, for example, A, γ, $\Delta\gamma$. We note θ_Y the wetting angle, defined by $\Delta\gamma + \gamma\cos\theta_Y = 0$, and we use θ_Y instead of $\Delta\gamma$ as parameter. We start with non-dimensionalizing the equilibrium equations. The configuration of the beam in the region $s \in (D; L]$ is trivial: the beam is straight, and there is no stress $\theta'(s) \equiv M(s) \equiv 0$ and $\nu_e(s) \equiv \lambda_e(s) \equiv 0$. The value of the length L is therefore of no importance, it can be anything as long as $L > D$. Consequently, we use $\sqrt{A}$ as unit length, and YI/A as unit force. The equilibrium equations for the dimensionless quantities (with over-tildes) read:

$$\tilde{x}'(\tilde{s}) = \cos\theta, \tilde{y}'(\tilde{s}) = \sin\theta, \tag{3.26a}$$

$$\theta''(\tilde{s}) = \tilde{n}_x \sin\theta - \tilde{n}_y \cos\theta \tag{3.26b}$$

and

$$\tilde{n}_x'(\tilde{s}) = -\left(\frac{\tilde{\gamma}}{\tilde{r}}\right)\sin\theta, \tilde{n}_y'(\tilde{s}) = \left(\frac{\tilde{\gamma}}{\tilde{r}}\right)\cos\theta, \tag{3.26c}$$

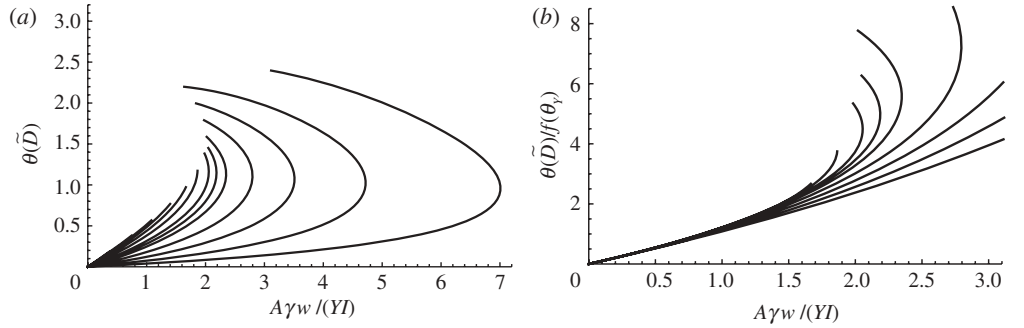

Figure 3. Inclination $\theta(\tilde{D})$ of a beam deformed by a liquid drop, in the absence of gravity. (*a*) $\theta(\tilde{D})$ as a function of the non-dimensionalized surface tension $\tilde{\gamma}$, for several value of the wetting angle θ_Y. (*b*) $\theta(\tilde{D})$ scaled with $f(\theta_Y)$, see formula (3.30). Near the origin, curves for different θ_Y collapse on a straight line of slope unity.

where $\tilde{\gamma} = A\gamma w/(YI)$ is a dimensionless quantity measuring the strength of surface tension. Volume conservation (3.3) now reads

$$1 = \tilde{r}^2\left(\beta - \frac{1}{2}\sin 2\beta\right) + 2\tilde{x}_D\tilde{y}_D - 2\int_0^{\tilde{D}} \tilde{y}\cos\theta \,\mathrm{d}\tilde{s}. \tag{3.27}$$

The boundary conditions at $s = 0$ are $\tilde{x}(0) = 0$, $\tilde{y}(0) = 0$ and $\theta(0) = 0$. The boundary conditions at $\tilde{s} = \tilde{D}$ are:

$$\tilde{x}(\tilde{D}) = \tilde{r}\sin\beta, \quad \theta'(\tilde{D}) = 0, \quad \tilde{n}_x(\tilde{D}) = -\tilde{\gamma}\cos\beta, \quad \tilde{n}_y(\tilde{D}) = \tilde{\gamma}\sin\beta, \quad \theta(\tilde{D}) + \beta = \theta_Y. \tag{3.28}$$

For each value of the fixed parameters $\tilde{\gamma}$ and θ_Y, we numerically solve this boundary value problem with a shooting method where the six unknowns $\theta'(0)$, $\tilde{n}_x(0)$, $\tilde{n}_y(0)$, β, $\tilde{D}$ and $\tilde{r}$ are balanced by the five boundary conditions (3.28) and the constraint (3.27). Results for the inclination of the beam at $\tilde{s} = \tilde{D}$ are plotted in figure 3*a*. We remark that equations (3.26*b*) and (3.26*c*) can be simplified to

$$\theta'(s) = -\frac{\tilde{\gamma}}{2r}y^2 + n_x(0)y - \frac{\tilde{\gamma}}{2r}x^2 - n_y(0)x + \theta'(0), \tag{3.29}$$

and boundary conditions (3.28) imply $\tilde{n}_y(0) = 0$.

We also look for analytical solutions when the surface tension is small $\tilde{\gamma} \ll 1$, that is when the elastocapillary length is large: $L_{\mathrm{ec}} = \sqrt{YI/(\gamma w)} \gg \sqrt{A}$. We develop unknowns in the power of $\tilde{\gamma}$: $\tilde{x}(\tilde{s}) = \tilde{x}_0(\tilde{s}) + \tilde{\gamma}\tilde{x}_1(\tilde{s}) + \cdots$, $\tilde{y}(\tilde{s}) = 0 + \tilde{\gamma}\tilde{y}_1(\tilde{s}) + \cdots$, $\theta(\tilde{s}) = 0 + \tilde{\gamma}\theta_1(\tilde{s}) + \cdots$, $\tilde{D} = \tilde{D}_0 + \tilde{\gamma}\tilde{D}_1 + \cdots$, etc. We find $\tilde{x}_0(\tilde{s}) = \tilde{s}$, $\theta_1(\tilde{s}) = \tilde{s}(3D^2 - \tilde{s}^2)/(6r)$ and $\tilde{y}_1(\tilde{s}) = \tilde{s}^2(6D^2 - \tilde{s}^2)/(24\tilde{r})$, $\beta_0 = \theta_Y$, $\tilde{D}_0 = \tilde{r}_0\sin\theta_Y$ and $1/\tilde{r}_0 = \sqrt{\theta_Y - \sin\theta_Y\cos\theta_Y}$. This yields:

$$\theta(\tilde{D}) = \frac{\tilde{\gamma}}{3}\frac{\sin^3\theta_Y}{\theta_Y - \sin\theta_Y\cos\theta_Y} + O(\tilde{\gamma}^2) = \tilde{\gamma}f(\theta_Y) + O(\tilde{\gamma}^2) \tag{3.30}$$

and

$$\tilde{y}(\tilde{D}) = \frac{5\tilde{\gamma}}{24}\frac{\sin^4\theta_Y}{(\theta_Y - \sin\theta_Y\cos\theta_Y)^{3/2}} + O(\tilde{\gamma}^2). \tag{3.31}$$

4. Liquid drop on a flexible beam, in the presence of gravity

We now consider the situation where gravity is no longer neglected. The beam has mass per length τ, and the weight of the beam introduces the term

$$\int_0^L \tau g y(s)\,\mathrm{d}s \tag{4.1}$$

in the potential energy (3.10). Yet, the main difference is that the liquid–air interface is no longer a circular-arc and its shape $y_{\mathrm{lv}}(x)$ has to be solved for. The liquid–air interface energy is now

$$\gamma w \int_0^{x(D)} \sqrt{1 + y'_{\mathrm{lv}}(x)^2}\, \mathrm{d}x + 2\gamma A. \tag{4.2}$$

In addition, the weight of the liquid (of density ρ) has to be accounted for, yielding the term:

$$\rho g w \int_0^{x(D)} \int_y^{y_{\mathrm{lv}}} y\, \mathrm{d}y\, \mathrm{d}x. \tag{4.3}$$

Finally, the constraint of constant volume now reads

$$A = \int_0^{x(D)} \int_y^{y_{\mathrm{lv}}} \mathrm{d}y\, \mathrm{d}x. \tag{4.4}$$

As carried out previously, the beam geometry is parametrized with the arc-length s: $x(s), y(s), \theta(s)$. As for the liquid–air interface, we introduce the relative height $h = y_{\mathrm{lv}} - y(D)$ and we parametrize it with the same variable s: $h(s) = h(x(s))$ (figure 4). The arc-length s along the beam is thus the unique independent variable. Dropping out constant terms in the energy, the Lagrangian of the system reads

$$\begin{aligned}\mathcal{L}(x, y, \theta, h, D) = {} & \frac{1}{2} YI \int_0^L [\theta'(s)]^2\, \mathrm{d}s + \int_0^L \tau g y\, \mathrm{d}s + wD\Delta\gamma + \gamma w \int_0^D \sqrt{x'^2 + h'^2}\, \mathrm{d}s \\ & + \rho g w \int_0^D \frac{1}{2}[(h + y(D))^2 - y^2]x'\, \mathrm{d}s - \mu w \int_0^D (h + y(D) - y)x'\, \mathrm{d}s \\ & + \int_0^D \nu_i(s)[x' - \cos\theta]\, \mathrm{d}s + \int_D^L \nu_e(s)[x' - \cos\theta]\, \mathrm{d}s \\ & + \int_0^D \lambda_i(s)[y' - \sin\theta]\, \mathrm{d}s + \int_D^L \lambda_e(s)[y' - \sin\theta]\, \mathrm{d}s. \end{aligned} \tag{4.5}$$

Boundary conditions are $x(0) = y(0) = \theta(0) = 0$, $h'(0) = 0$ and $h(D) = 0$. As in §3, we note $X = (x, y, \theta, h, D)$ and we look for X_e such that the first variation $\mathcal{L}'(X_e)(\bar{X})$ vanishes when X is changed from X_e to $X_e + \epsilon\bar{X}$. We compute the first variation of $\mathcal{L}$ with regard to the variable $X = (x, y, \theta, h, D)$:

$$\begin{aligned}\mathcal{L}'(X_e)(\bar{X}) = {} & YI \int_0^L \theta'\bar{\theta}'\, \mathrm{d}s + \int_0^L \tau g \bar{y}\, \mathrm{d}s + w\bar{D}\Delta\gamma + \gamma w \int_0^D \frac{x'\bar{x}' + h'\bar{h}'}{\sqrt{x'^2 + h'^2}}\, \mathrm{d}s + \bar{D}\gamma w \sqrt{x'(D)^2 + h'(D)^2} \\ & + \rho g w \int_0^D \Big\{ h\bar{h}x' + h\bar{y}(D)x' + hy'(D)\bar{D}x' + \bar{h}y(D)x' + y(D)\bar{y}(D)x' \\ & + \bar{D}y(D)y'(D)x' - y\bar{y}x' + \frac{1}{2}[(h + y(D))^2 - y^2]\bar{x}' \Big\}\, \mathrm{d}s \\ & - \mu w \int_0^D [(\bar{h} + \bar{y}(D) + \bar{D}y'(D) - \bar{y})x' + (h + y(D) - y)\bar{x}']\, \mathrm{d}s \\ & + \int_0^D \nu_i(s)[\bar{x}' + \bar{\theta}\sin\theta]\, \mathrm{d}s + \int_D^L \nu_e(s)[\bar{x}' + \bar{\theta}\sin\theta]\, \mathrm{d}s \\ & + \int_0^D \lambda_i(s)[\bar{y}' - \bar{\theta}\cos\theta]\, \mathrm{d}s + \int_D^L \lambda_e(s)[\bar{y}' - \bar{\theta}\cos\theta]\, \mathrm{d}s. \end{aligned} \tag{4.6}$$

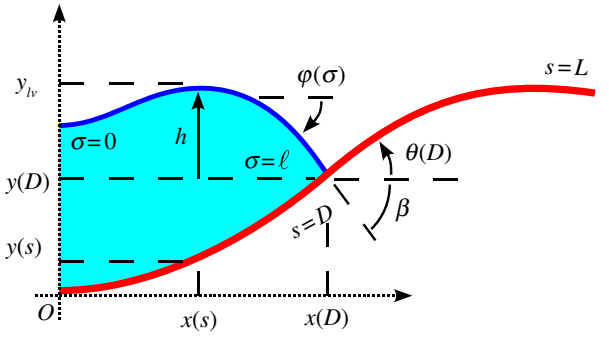

Figure 4. A flexible beam bent by a liquid drop, in the presence of gravity. Owing to symmetry, we consider only positive x's. (Online version in colour.)

We now require the first variation to vanish for all $\bar{x}, \bar{y}, \bar{\theta}, \bar{h}$ and $\bar{D}$. Collecting terms involving $\bar{h}$ and $\bar{h}'$ yields, after integration by parts:

$$\gamma w\left[\frac{h'\bar{h}}{\sqrt{x'^2+h'^2}}\right]_0^D+\int_0^D\left(-\gamma w\left(\frac{h'}{\sqrt{x'^2+h'^2}}\right)'+\rho g w(h+y(D))x'-\mu w x'\right)\bar{h}\,\mathrm{d}s. \tag{4.7}$$

The first term is $\gamma w h'(D)\bar{h}(D)/\sqrt{x'(D)^2+h'(D)^2}$. Boundary conditions require that $h+\epsilon\bar{h}$ vanishes at $s=D+\epsilon\bar{D}$; this yields $\bar{h}(D)=-\bar{D}h'(D)$. Consequently, this first term effectively goes into the equation for $\bar{D}$, see (4.10). The second term of (4.7) has hence to vanish for all $\bar{h}(s)$, which implies that the liquid–air interface $h(s)$ obeys the equation:

$$[\rho g w(h+y(D))-\mu w]x'=\gamma w\left(\frac{h'}{\sqrt{x'^2+h'^2}}\right)'. \tag{4.8}$$

Integrating this equation from $s=0$ to $s=D$ yields

$$\rho g w\hat{A}-\mu w x(D)=\gamma w\sin\varphi(D), \tag{4.9}$$

where $\hat{A}=\int_0^D(h+y(D))x'\,\mathrm{d}s$ is the area between the liquid–air interface and the horizontal axis, and where φ is the angle the interface makes with the horizontal. Evaluating (4.8) at $s=0$ reveals that the Lagrange multiplier μ is the hydrostatic pressure at the origin.

Requiring (4.6) to vanish for all $\bar{D}$ yields

$$w\Delta\gamma+w\gamma\sqrt{x'(D)^2+h'(D)^2}-w\gamma\frac{h'(D)^2}{\sqrt{x'(D)^2+h'(D)^2}}+y'(D)(\rho g w\hat{A}-\mu w x(D))=0. \tag{4.10}$$

Using $x'(D)/\sqrt{x'(D)^2+h'(D)^2}=\cos\varphi(D)$, $x'(D)=\cos\theta(D)$, $y'(D)=\sin\theta(D)$, and (4.9) we arrive at:

$$\Delta\gamma+\gamma\cos[\theta(D)+\beta]=0, \tag{4.11}$$

where $\beta=-\varphi(D)$. This is Young–Dupré relation for the wetting angle $\theta(D)+\beta$. We collect terms involving $\bar{x}$ and $\bar{x}'$ in (4.6) and we integrate by parts to obtain:

$$\begin{aligned}&\left[\left\{\frac{w\gamma x'}{\sqrt{x'^2+h'^2}}+\frac{1}{2}\rho g w(h+y(D))^2-\frac{1}{2}\rho g w y^2+v_i-\mu w(h+y(D)-y)\right\}\bar{x}\right]_0^D\\&-\int_0^D\left\{\left(\frac{w\gamma x'}{\sqrt{x'^2+h'^2}}\right)'+\rho g w(h+y(D))h'-\rho g w y y'-\mu w(h'-y')+v_i'\right\}\bar{x}\,\mathrm{d}s\\&+[v_e\bar{x}]_D^L-\int_D^L v_e'\bar{x}\,\mathrm{d}s=0.\end{aligned} \tag{4.12}$$

The fact that we have $\bar{x}(0) = 0$, but arbitrary $\bar{x}(D)$ and $\bar{x}(L)$ implies

$$\nu_e(L) = 0, \tag{4.13}$$

$$\nu_e'(s) = 0, \tag{4.14}$$

$$\nu_e(D) - \nu_i(D) = \frac{w\gamma x'(D)}{\sqrt{x'(D)^2 + h'(D)^2}} = w\gamma \cos\varphi(D) = w\gamma \cos\beta \tag{4.15}$$

and

$$\nu_i' = -(\mu w - \rho g w y)y' - [\rho g w(h + y(D)) - \mu w]h' - \gamma w \left(\frac{x'}{\sqrt{x'^2 + h'^2}}\right)'. \tag{4.16}$$

Considering the identity $x'(x'/\sqrt{x'^2 + h'^2})' + h'(h'/\sqrt{x'^2 + h'^2})' = 0$ and (4.8), equation (4.16) reduces to

$$\nu_i' = -(\mu w - \rho g w y)y'. \tag{4.17}$$

Requiring (4.6) to vanish for all $\bar{y}$ similarly yields, after the use of (4.9):

$$\lambda_e(L) = 0, \lambda_e(D) - \lambda_i(D) = -w\gamma \sin\beta \tag{4.18}$$

and

$$\lambda_e' = \tau g, \lambda_i' = \tau g + (\mu w - \rho w g y)x'. \tag{4.19}$$

Finally, requiring (4.6) to vanish for all $\bar{\theta}$ yields the same equation as before, see equations (3.20) and (3.21).

From (4.15) and (4.18), we see that the internal force experiences the same discontinuity as in the case without gravity (3.25): here also the external force applied on the beam at $s = D$ is along the meniscus.

(a) Equilibrium solutions

We now solve the boundary value problem for different values of the parameters, for example, A, γ, $\Delta\gamma$, τ. We note θ_Y the wetting angle, defined by $\Delta\gamma + \gamma\cos\theta_Y = 0$, and we use θ_Y instead of $\Delta\gamma$ as parameter. We start with non-dimensionalizing the equilibrium equations. As the configuration of the beam in the region $s \in (D; L]$ is no longer trivial, we use L as unit length, EI/L^2 as unit force, and EI/L as unit moment. For the beam, the equilibrium equations for the dimensionless quantities (with over-tildes) read

$$\tilde{x}'(\tilde{s}) = \cos\theta, \quad \tilde{y}'(\tilde{s}) = \sin\theta, \tag{4.20a}$$

$$\theta''(\tilde{s}) = \tilde{n}_x \sin\theta - \tilde{n}_y \cos\theta \tag{4.20b}$$

and

$$\tilde{n}_x'(\tilde{s}) = -P\sin\theta, \quad \tilde{n}_y'(\tilde{s}) = \tilde{\tau} + P\cos\theta, \tag{4.20c}$$

where P is the dimensionless hydrostatic pressure $P = (L/L_{ec})^2[\tilde{\mu} - (L/L_c)^2\tilde{y}]$ for the region $\tilde{s} \in [0; \tilde{D})$ and $P = 0$ for $\tilde{s} > \tilde{D}$. We have introduced the dimensionless pressure $\tilde{\mu} = \mu L/\gamma$, the capillary length $L_c = \sqrt{\gamma/(\rho g)}$ and the elastocapillary length $L_{ec} = \sqrt{YI/(\gamma w)}$ [12].

The equations for the liquid–air interface (4.8) can be rewritten using (i) the angle φ the interface does with the horizontal, and (ii) the arc-length σ along this interface:

$$\varphi'(\tilde{\sigma}) = \left(\frac{L}{L_c}\right)^2 [\tilde{h} + \tilde{y}(\tilde{D})] - \tilde{\mu} \tag{4.21a}$$

and

$$\tilde{h}'(\tilde{\sigma}) = \sin\varphi, \quad \tilde{\xi}'(\tilde{\sigma}) = \cos\varphi, \tag{4.21b}$$

where $\tilde{\sigma} = \sigma/L$. The liquid–air interface has total contour length ℓ.

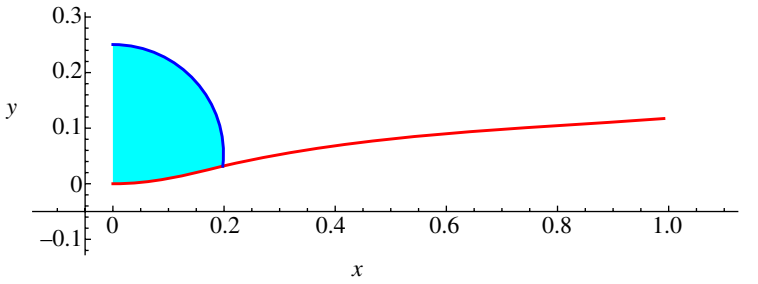

Figure 5. A flexible beam bent by a liquid drop, in the presence of gravity. (Online version in colour.)

As soon as values for the fixed parameter L_{ec}/L, L_c/L, $\tilde{\tau}$, $\tilde{A}$ and θ_Y are given, the boundary value problem can be solved with a shooting procedure, where $\theta'(0)$, $\tilde{n}_x(0)$, $\tilde{n}_y(0)$, $\tilde{\mu}$, $\tilde{h}(0)$, $\tilde{D}$, $\tilde{\ell}$ are seven unknowns. Integration of (4.20) is performed for $\tilde{s} \in [0;\tilde{D})$, and integration of (4.21) is performed for $\tilde{\sigma} \in [0;\tilde{\ell}]$. At $\tilde{s} = \tilde{D}$, a jump in the force vector is introduced according to (4.15) and (4.18) with $\beta = -\varphi(\tilde{\ell})$ and $n_x = \nu$, $n_y = \lambda$. Then, integration of (4.20) is performed for $\tilde{s} \in (\tilde{D};1)$. Seven boundary equations have then to be fulfilled

$$\theta'(1) = 0, \quad \tilde{n}_x(1) = 0, \quad \tilde{n}_y(1) = 0, \quad \tilde{h}(\tilde{\ell}) = 0, \quad \tilde{\xi}(\tilde{\ell}) = \tilde{x}(\tilde{D}), \quad \theta(\tilde{D}) + \beta = \theta_Y \tag{4.22}$$

together with the volume condition

$$\tilde{A} = \int_0^{\tilde{\ell}} \tilde{h} \cos\varphi \, \mathrm{d}\tilde{\sigma} - \int_0^{\tilde{D}} [\tilde{y} - \tilde{y}(\tilde{D})] \cos\theta \, \mathrm{d}\tilde{s}. \tag{4.23}$$

A solution for $L_{ec}/L = 0.175$, $L_c/L = 0.982$, $\tilde{\tau} = 2$, $\tilde{A} = 0.039$ and $\theta_Y = 110^\circ$ is shown in figure 5. The seven unknowns of the shooting procedure are found to be $\theta'(0) = 1.887$, $\tilde{n}_x(0) = 9.15$, $\tilde{n}_y(0) = -3.32$, $\tilde{\mu} = 5.24$, $\tilde{h}(0) = 0.219$, $\tilde{D} = 0.201$ and $\tilde{\ell} = 0.333$.

5. Pinning, receding and advancing of the contact line

We now turn to the case of contact line pinning and we show, following Alberti & DeSimone [13], that pinning, receding and advancing of the contact line can be treated in a variational approach where irreversibility conditions are introduced. We consider the drop of figure 1, lying at equilibrium on a rigid substrate with its contact angle β equal to the Young–Dupré angle θ_Y, defined by $\Delta\gamma + \gamma\cos\theta_Y = 0$, $\beta(t=0) = \theta_Y$. At time $t = 0$, evaporation starts to take place, and we study the subsequent behaviour of the drop. In the absence of contact line pinning, the contact angle β will stay at $\beta(t) = \theta_Y$, and the wetted length D will decrease in order to keep on fulfilling the volume constraint. In the presence of contact line pinning, the length D will first stay fixed, and the contact angle β will decrease: $\beta(t > 0) < \theta_Y$ to fulfill the volume constraint. Eventually, as $\beta(t)$ reaches a receding threshold, the contact line will start to move: $D = D(t)$.

As in §2 we start with the interfaces energies, equation (2.1), and we use the constraint $D = r\sin\beta$ to eliminate the variable r: per unit w, the energy is $2\gamma D\beta/\sin\beta + 2D\Delta\gamma$. As D decreases from $D(t=0)$, receding of the contact line is associated with an energy dissipation $k > 0$ per unit area [14,15], which we introduce in the energy:

$$E(D,\beta) = 2\gamma D\frac{\beta}{\sin\beta} + 2D\Delta\gamma + k(D(0) - D). \tag{5.1}$$

At each time step $t = t_i$, we look for the equilibrium of the drop with a fixed volume, hence we still minimize this energy under the constraint $V(t_i)/w = r^2(\beta - \sin\beta\cos\beta) = (D/\sin\beta)^2(\beta - \sin\beta\cos\beta)$. At the next time step t_{i+1}, the volume constraint remains, but the imposed volume $V(t_{i+1})$ is smaller than $V(t_i)$. Moreover, we introduce the irreversibility condition $D(t_{i+1}) \leq D(t_i)$,

which we note $D \leq D^-$ and finally write the Lagrangian:

$$\mathcal{L} = E(D,\beta) - \lambda(D^- - D) - \mu D^2 \left(\frac{\beta}{\sin^2 \beta} - \frac{\cos \beta}{\sin \beta} \right), \tag{5.2}$$

where μ is the Lagrange multiplier associated with the volume equality constraint, and where λ is the Lagrange multiplier associated with the inequality constraint $D \leq D^-$. The necessary conditions for having a minimum are:

$$\frac{\partial \mathcal{L}}{\partial \beta} = 0 \Rightarrow \mu D = \gamma \sin \beta, \tag{5.3}$$

$$\frac{\partial \mathcal{L}}{\partial D} = 0 \Rightarrow 2\gamma \cos \beta + 2\Delta\gamma - k + \lambda = 0 \tag{5.4}$$

and

$$\text{KT} \Rightarrow \lambda \geq 0, (D^- - D) \geq 0, \quad \text{and} \quad \lambda(D^- - D) = 0, \tag{5.5}$$

where the last line lists the classical Kuhn–Tucker (KT) conditions [16] arising in the case of inequality constraints. These three conditions express the fact that either the pinning force λ is zero and sliding occurs $D < D^-$, or the pinning force is strictly positive $\lambda > 0$ preventing the contact line to move: $D = D^-$. We now introduce an angle $\theta^\star$ such that $2(\Delta\gamma + \gamma \cos \theta^\star) = k$. Positivity of the dissipation k implies that $\theta^\star < \theta_Y$. Equation (5.4) becomes $2\gamma(\cos \beta - \cos \theta^\star) + \lambda = 0$ and eliminating λ in (5.5), we finally obtain:

$$\cos \theta^\star - \cos \beta \geq 0, \tag{5.6a}$$

$$D^- - D \geq 0 \tag{5.6b}$$

and

$$(\cos \theta^\star - \cos \beta)(D^- - D) = 0 \tag{5.6c}$$

which means that either D is fixed to D^- and $\beta > \theta^\star$ (contact line pinning) or $\beta = \theta^\star$ and D decreases $D < D^-$ (contact line sliding, here receding or dewetting), as was used in Rivetti & Neukirch [6].

Note that for the sake of simplicity we have presented only equations for receding of the contact line, but the present treatment can be performed for the general case where advancing and receding can both occur (see [17]).

(a) Illustration

We here illustrate the present theory on an imaginary experiment where one deposits a drop on an elastic strip (figure 4) and wait for evaporation to take place [4,18]. After deposition, the drop contact angle $\theta(D) + \beta$ takes some intermediate value between receding ($\theta^\star$) and advancing values. We fix parameters $L_{ec} = 0.2L$, $L_c = 0.8L$ and $\tilde{\tau} = 1.4$, and we first solve equations (4.20)–(4.23) for several values of the receding angle $\theta^\star$ in the sliding hypothesis $\theta(D) + \beta = \theta^\star$. We then solve the equations for several values of $D(0)$ in the pinning hypothesis $D = D(0)$. Results are shown in figure 6.

In a typical experiment, starting at $\tilde{A} = A/L^2 = 0.14$ with $D(0)/L = 0.26$, evaporation first results in the decrease of the contact angle, following the curve C_{D1} in figure 7. As the contact angle $\theta(D) + \beta$ reaches $\theta^\star$ (with say $\theta^\star = 2$), the system switches branch at point P_1 and follows the constant contact angle curve C_θ down to $\tilde{A} = 0$. This branching can be understood by looking at energy curves. In figure 7*b*, we plot the energy as given by the first five terms of (4.5) supplemented by the dissipation term $-kwD$, with $k = \Delta\gamma + \gamma \cos \theta^\star$. At point P_1 and going towards small A, the energy on curve C_θ is seen to be smaller than the energy on C_{D1}. If now one starts at $\tilde{A} = 0.14$ with $D(0)/L = 0.43$, during evaporation, then the system follows curve C_{D2} down to point P_2. We note that in the neighbourhood of point P_2 the energy on curve C_θ is larger than the energy on curve C_{D2}. Moreover, in the neighbourhood of P_2, configurations on C_θ are unstable. We suggest that at P_2 the system jumps to another configuration, with same volume. Such a configuration might be on the stable part of curve C_θ, or might be a configuration with $x(L) = 0$, where the extremities of the beam contact.

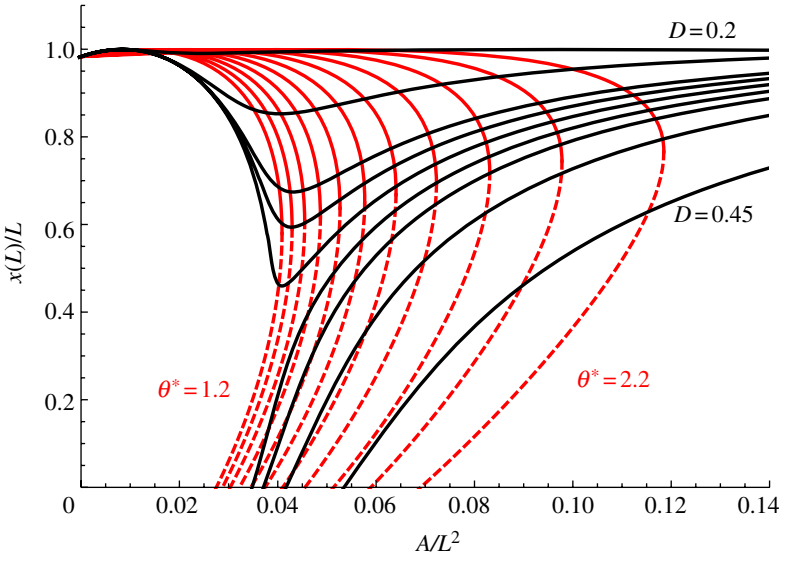

Figure 6. Bifurcation diagram for the system of figure 4 with $L_{ec} = 0.2L$, $L_c = 0.8L$ and $\tilde{\tau} = 1.4$. The first set of 11 (red or grey) curves correspond to equilibrium in the sliding hypothesis $\theta(D) + \beta = \theta^\star$, with $\theta^\star = 1.2, 1.3, \ldots, 2.2$. These curves all have a limit point for the variable $\tilde{A} = A/L^2$. Dashed parts of the curves correspond to unstable equilibria. The second set of 10 (black) curves correspond to equilibrium in the pinning hypothesis $D = D(0)$, with $D(0)/L = 0.2, 0.3, 0.32, 0.34, 0.35, 0.36, 0.37, 0.38, 0.4, 0.45$. (Online version in colour.)

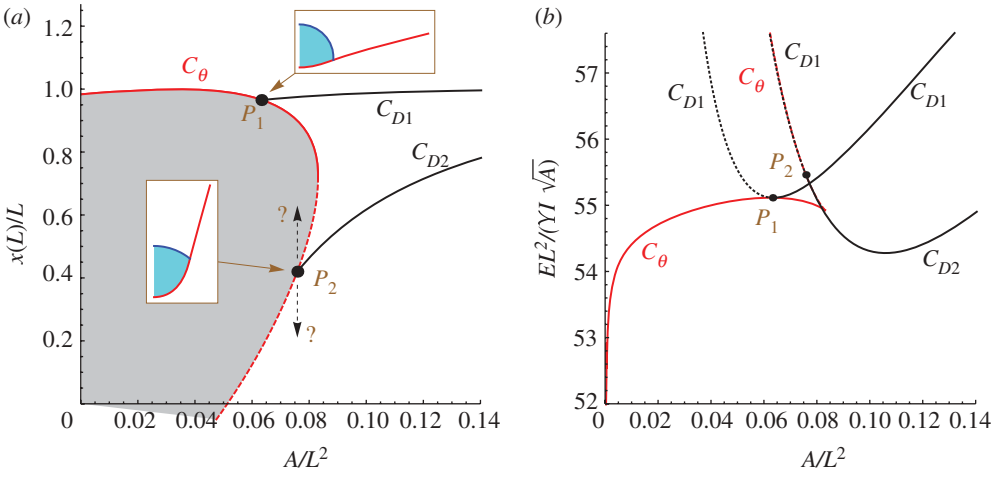

Figure 7. Evaporation experiment with $L_{ec} = 0.2L$, $L_c = 0.8L$ and $\tilde{\tau} = 1.4$. The curve C_θ corresponds to equilibrium in the sliding hypothesis $\theta(D) + \beta = \theta^\star$ with $\theta^\star = 2$. The curves C_{D1} and C_{D2} correspond to equilibrium in the pinning hypothesis $D = D(0)$, with $D(0)/L = 0.26$ and 0.43, respectively. (*a*) Horizontal position $x(L)$ of the tip of the beam as function of the drop volume V, with $A = V/w$. The region $\theta(D) + \beta < 2$ is shown shaded. If evaporation starts on C_{D1} at $A/L^2 = 0.14$, then the system reaches point P_1 and then follows the upper part of curve C_θ down to $A = 0$. (*b*) Energy of the system as function of the drop volume. We see that as the system goes through point P_1, it chooses the branch with the minimum energy. If evaporation starts on C_{D2} at $A/L^2 = 0.14$, then the system reaches point P_2. There, configurations on C_θ are unstable and have higher energy. Consequently, the system jumps to a configuration with the same value of A, discussed in the main text. (Online version in colour.)

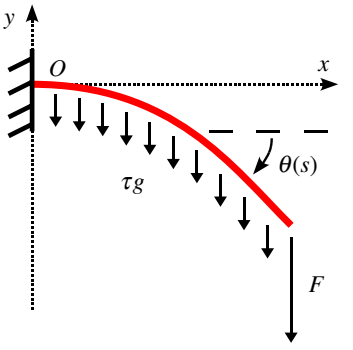

Figure 8. Cantilever beam sagging under the combined actions of its own weight τg and of a localized shear force F at its left end. (Online version in colour.)

6. Conclusion

In conclusion, we have recalled that the classical Young–Dupré relation for the contact angle of a drop lying on a rigid substrate can be derived from a variational approach where the concept of force is not invoked. The variational approach has then been extended to the case where the substrate is a flexible beam, and we have shown that the Young–Dupré relation still holds. Moreover, provided that Lagrange multipliers introduced in the variational formulation can be identified with internal force components in the beam, we have found that the external force applied on the elastic beam at the triple point is tangential to the liquid–vapour interface. We then extended the approach to the case where gravity is included and found that these two results continue to hold. The present result showing that in the case a flexural deformations the external force on the elastic beam is along the meniscus is in contradiction to what is found in Marchand *et al.* [7] in the case of extensional deformations. Namely Marchand *et al.* [7] suggest that a supplementary force is acting at the meniscus, along the tangent to the beam. Such a tangential point force would typically generate extensional deformations, not considered in our present model. We therefore conclude that extensional deformations have to be introduced in our variational formulation before we can further investigate this discrepancy.

Finally, we have shown how contact line pinning can be dealt with in the variational formulation and we have illustrated our model with the study of the evaporation of a drop deposited on a flexible beam and have shown that, depending on the initial spreading of the drop on the beam, evaporation might lead to a flat or a folded system.

Acknowledgements. We thank Giovanni Alberti and Antonio De Simone for reminding us of Gauss' work [8].

Funding statement. The present work was supported by ANR grant (no. ANR-09-JCJC-0022-01). Financial support from 'La Ville de Paris-Programme Émergence' is also gratefully acknowledged.

Appendix A. Planar elastica

The equilibrium equations for the system in figure 8 are [19,20]

$$x'(s) = \cos\theta, y'(s) = \sin\theta, \tag{A 1a}$$

$$YI\theta'(s) = M, M'(s) = N_x \sin\theta - N_y \cos\theta \tag{A 1b}$$

and

$$N_x'(s) = -p_x^{\text{ext}}, N_y'(s) = -p_y^{\text{ext}}, \tag{A 1c}$$

where s is the arc-length of the beam, M is the internal bending moment, $N = (N_x, N_y)$ is the internal force, (x, y) is the current position of the central line and θ is the angle between the tangent of the centre line and the horizontal axis. The bending moment is linearly related to the curvature

$\theta'(s)$ through the bending rigidity YI, where Y is Young's modulus and I is the second moment of area of the beam cross section. In the case of a rectangular cross section of thickness h and width w, $I = h^3 w/12$ when bending occurs in the plane of the thickness h. The beam is clamped at $s = 0$, and a vertical force $(0, -F)$ is applied at the $s = L$ extremity. We also consider the self-weight of the beam $p^{\text{ext}} = (0, -\tau g)$, where τ is the mass per unit arc-length of the beam. The left boundary conditions are $x(0) = 0$, $y(0) = 0$, $\theta(0) = 0$, and the right boundary conditions are $N_x(L) = 0$, $N_y(L) = -F$ and $M(L) = 0$.

The equilibrium equations can be recovered by considering the energy:

$$E = \frac{1}{2} YI \int_0^L [\theta']^2 \, \mathrm{d}s + \tau g \int_0^L y \, \mathrm{d}s + Fy(L), \tag{A 2}$$

and the Lagrangian

$$\mathcal{L}(x, y, \theta) = E + \int_0^L \nu_i(s)[x' - \cos\theta] \, \mathrm{d}s + \int_0^L \lambda_i(s)[y' - \sin\theta] \, \mathrm{d}s \tag{A 3}$$

subjected to the left boundary conditions. The conditions for the vanishing of the first variation of the Lagrangian will yield the equilibrium equations (A 1) together with the right boundary conditions [21].

References

1. Syms R, Yeatman E, Bright V, Whitesides G. 2003 Surface tension-powered self-assembly of microstructures: the state-of-the-art. *J. Microelectromech. Syst.* **12**, 387–417. (doi:10.1109/JMEMS.2003.811724)
2. Marchand A, Weijs JH, Snoeijer JH, Andreotti B. 2011 Why is surface tension a force parallel to the interface? *Am. J. Phys.* **79**, 999–1008. (doi:10.1119/1.3619866)
3. Roman B, Bico J. 2010 Elasto-capillarity: deforming an elastic structure with a liquid droplet. *J. Phys. Condensed Matter* **22**, 493101. (doi:10.1088/0953-8984/22/49/493101)
4. Py C, Reverdy P, Doppler L, Bico J, Roman B, Baroud CN. 2007 Capillary origami: spontaneous wrapping of a droplet with an elastic sheet. *Phys. Rev. Lett.* **98**, 156103. (doi:10.1103/PhysRevLett.98.156103)
5. Antkowiak A, Audoly B, Josserand C, Neukirch S, Rivetti M. 2011 Instant fabrication and selection of folded structures using drop impact. *Proc. Natl Acad. Sci. USA* **108**, 10 400–10 404. (doi:10.1073/pnas.1101738108)
6. Rivetti M, Neukirch S. 2012 Instabilities in a drop–strip system: a simplified model. *Proc. R. Soc. A* **468**, 1304–1324. (doi:10.1098/rspa.2011.0589)
7. Marchand A, Das S, Snoeijer JH, Andreotti B. 2012 Capillary pressure and contact line force on a soft solid. *Phys. Rev. Lett.* **108**, 094301. (doi:10.1103/PhysRevLett.108.094301)
8. Gauss C. 1830 *Principia generalia theoriae figurae fluidorum in statu aequilibrii*. Göttingae, Germany: Dieterichs. (Reprinted; Nabu Press, 2010)
9. Gauss CF. 1877 *Werke*, vol. 5. Göttingen, Germany: Königliche Gesellschaft der Wissenschaften.
10. Kirchhoff G. 1876 *Vorlesungen über mathematische Physik, Mechanik*. Leipzig, Germany: B. G. Teubner.
11. Neukirch S, Roman B, de Gaudemaris B, Bico J. 2007 Piercing a liquid surface with an elastic rod: buckling under capillary forces. *J. Mech. Phys. Solids* **55**, 1212–1235. (doi:10.1016/j.jmps.2006.11.009)
12. Bico J, Roman B, Moulin L, Boudaoud A. 2004 Adhesion: elastocapillary coalescence in wet hair. *Nature* **432**, 690. (doi:10.1038/432690a)
13. Alberti G, DeSimone A. 2011 Quasistatic evolution of sessile drops and contact angle hysteresis. *Arch. Ration. Mech. Anal.* **202**, 295–348. (doi:10.1007/s00205-011-0427-x)
14. Joanny JF, de Gennes PG. 1984 A model for contact angle hysteresis. *J. Chem. Phys.* **81**, 552–562. (doi:10.1063/1.447337)
15. Alberti G, DeSimone A. 2005 Wetting of rough surfaces: a homogenization approach. *Proc. R. Soc. A* **461**, 79–97. (doi:10.1098/rspa.2004.1364)

16. Luenberger DG. 1973 *Introduction to linear and nonlinear programming*. London, UK: Addison-Wesley.
17. Fedeli L, Turco A, DeSimone A. 2011 Metastable equilibria of capillary drops on solid surfaces: a phase field approach. *Contin. Mech. Thermodyn.* **23**, 453–471. (doi:10.1007/s00161-011-0189-6)
18. de Langre E, Baroud C, Reverdy P. 2010 Energy criteria for elasto-capillary wrapping. *J. Fluids Struct.* **26**, 205–217. (doi:10.1016/j.jfluidstructs.2009.10.004)
19. Love AEH. 1944 *A treatise on the mathematical theory of elasticity*, 4th edn. New York, NY: Dover Publications.
20. Antman SS. 2004 *Nonlinear problems of elasticity*. New York, NY: Springer.
21. Audoly B, Pomeau Y. 2010 *Elasticity and geometry: from hair curls to the non-linear response of shells*. Oxford, UK: Oxford University Press.